Proceedings of the 30th International Cosmic Ray Conference
Rogelio Caballero, Juan Carlos D'Olivo, Gustavo Medina-Tanco,
Lukas Nellen, Federico A. Sánchez, José F. Valdés-Galicia (eds.)
Universidad Nacional Autónoma de México,
Mexico City, Mexico, 2008
Vol. 1 (SH), pages 737–740

ID 730

30TH INTERNATIONAL COSMIC RAY CONFERENCE

World Grid of Calculated Cosmic Ray Vertical Cutoff Rigidities for Epoch 2000.0

D.F. SMART[1], M.A. SHEA[1]
[1]*Emeritus at Air Force Research Laboratory (VSBX), Hanscom AFB, Bedford, MA, 01731, USA*
sssrc@msn.com

Abstract: A world grid of vertical cosmic ray cutoff rigidities was calculated using the International Geomagnetic Reference Field (IGRF) for Epoch 2000.0. These cutoff rigidity values, specifically computed for updating aircraft radiation dose, show the effects of the continued evolution of the geomagnetic field. The average cutoff values continue to decrease especially in the South Atlantic and South American areas. However, in the North Atlantic and the east coast of the North American continent, the cutoff values are increasing.

Introduction

We have continued to determine cosmic-ray cutoff rigidities by the trajectory-tracing method whereby the orbit of a particle of specified rigidity is traced, by numerical methods, through a model of the geomagnetic field to determine if the particle is allowed or forbidden for a specific zenith and azimuth at a given location. We have derived a world grid of vertically incident cosmic ray cutoff rigidities employing the 9^{th} generation of the International Geomagnetic Reference Field [1] for Epoch 2000. Geomagnetic cutoff rigidities were calculated each 5° in latitude and 5° in longitude so that a comparison can be made between these values and the values calculated for previous epochs.

Method

The cosmic ray trajectory calculations were initiated in the "vertical" direction at an altitude of 20 km above the surface of the international reference ellipsoid. Our standard cosmic ray trajectory-tracing technique was used employing the step size criteria where the length of each iteration step is about 1% of a gyro-distance (the distance the particle of the specified rigidity would travel during one gyration in a uniform magnetic field of the same intensity). The cutoff rigidities are determined by calculating cosmic ray trajectories at discrete rigidity intervals starting with a rigidity value high above the highest possible cutoff and decreasing the rigidity to a value that satisfied our criteria that the lowest allowed trajectory had been calculated. As a result of these trajectory calculations we determined the calculated upper cutoff rigidity (R_U), the calculated lower cutoff rigidity (R_L), and an "effective cutoff rigidity" (R_C) by summing over the allowed orbits in the penumbra. See Smart and Shea [2] (this conference) for more details describing the trajectory-tracing process and the cutoff determination process. See [3] for a definition of cosmic ray cutoffs.

Results and Discussion

These results are intended to be a reference for evaluating the effects attributable to the quiescent internal geomagnetic field. Figure 1 illustrates a world map of the effective vertical cutoff rigidities calculated for a world grid utilizing the IGRF model for Epoch 2000.0. A reduced (for the lack of space) 5° in latitude by 30° in longitude tabulation of these effective cutoffs is given in Table 1. When these values are compared with those calculated for previous epochs we find significant differences and non-linear changes, continuing the trends previously noted [4]. Figure 2 illustrates the long term change in the main dipole term. Decreases in vertical cutoff rigidity were found for many grid points in the eastern part of the Pacific Ocean area, over South America, and the South Atlantic ocean. Figure 3 illustrates the vertical cutoff rigidity changes (in GV) from 1950 to 2000. The cutoffs in the South Atlantic region continue to decrease at a rate of the order of 0.5% per year over a wide area. The largest decrease, 2.2 GV over the last 50 years is in the South Atlantic Ocean area around 25° S, 330° E. However, there are some areas where the vertical cutoff rigidities are increasing. The maximum increase over the last 50 years is in the North Atlantic Ocean area, an increase of 3 GV at 30° N, 315° E.

Conclusions

The vertical cutoff rigidities for Epoch 2000.0 continues to show significant and systematic changes from the previous epochs. With modern high speed computers it is now possible to re-calculate specific cutoff rigidities utilizing the updated International Geomagnetic Reference Field (IGRF) models for a specific epoch.

Acknowledgments

These calculations were performed at the Maui High Performance Computer Center.

References

[1] S. Macmillan, S. Maus, T. Bondar, et al., The 9th generation international geomagnetic reference field, Geophys. J. Int., 155, 1051-1056, 2003; URL:http://www.ngdc. noaa. gov /IAGA/vmod/igrf.html

[2] D.F. Smart, M.A. Shea, World grid of calculated cosmic ray vertical cutoff rigidities for epoch 1995.0, *30th ICRC*, this volume, 2007.

[3] D.J. Cooke, et al., On Cosmic-Ray Cut-Off Terminology, Il Nuovo Cimento C, 14, 213-234, 1991.

[4] M.A. Shea, D.F. Smart, Secular changes in the geomagnetic cutoff rigidities and the effect on cosmic ray measurements, 25th ICRC, 2, 393-396, 1997.

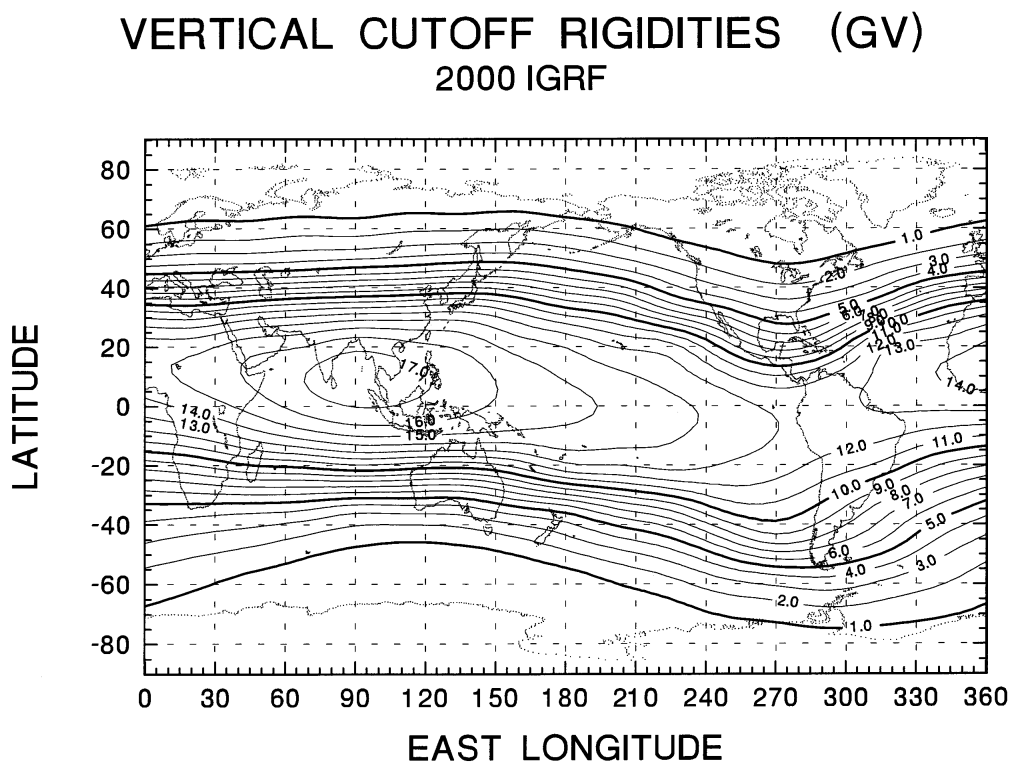

Figure 1: Iso-rigidity contours for vertical geomagnetic cutoff rigidities for epoch 2000.

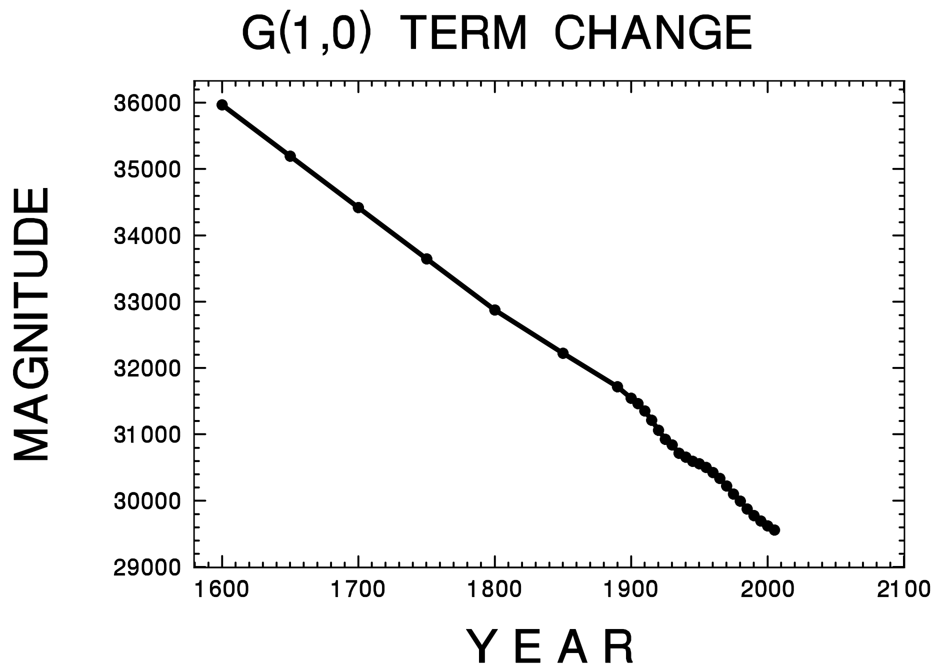

Figure 2: Change in magnitude of the Earth's dipole as represented by the G(1,0) term.

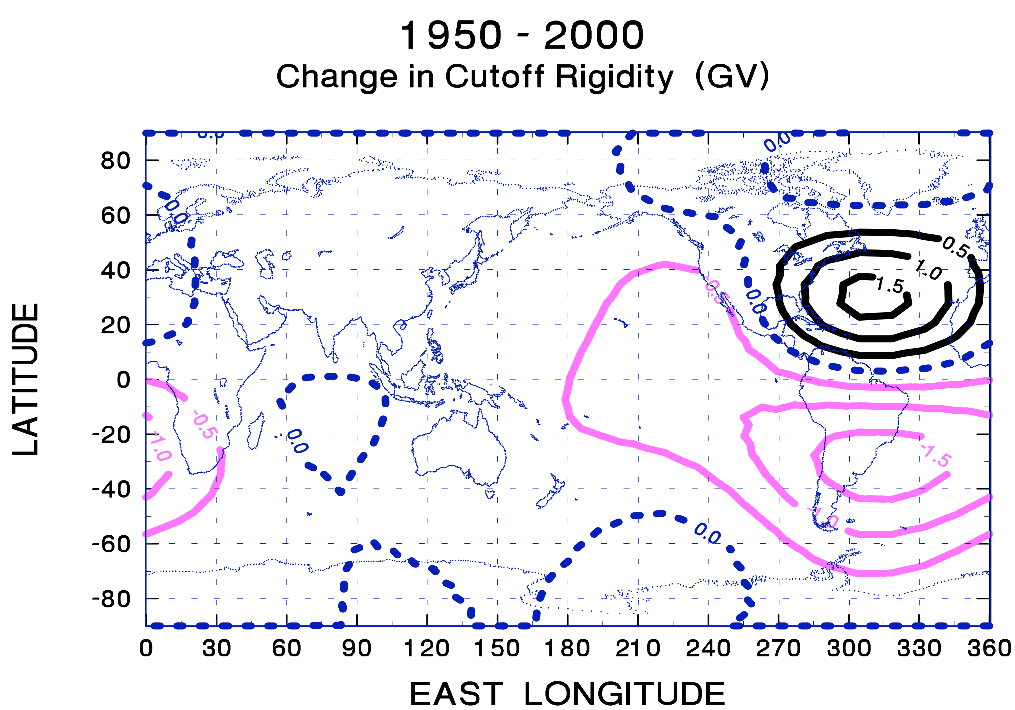

Figure 3: A map of the change in vertical cutoff rigidity (in units of GV) between 1950 and 2000. (Black indicates increase, Red indicates decrease).

Table 1: Effective Vertical Cutoff Rigidities (in GV) for Epoch 2000.0

	World Grid IGRF 2000					Geographic East Longitude						
	0	**30**	**60**	**90**	**120**	**150**	**180**	**210**	**240**	**270**	**300**	**330**
Lat												
90	0.00	0.00	0.00	0.00	0.00	0.00	0.00	0.00	0.00	0.00	0.00	0.00
85	0.00	0.00	0.00	0.00	0.00	0.00	0.00	0.00	0.00	0.00	0.00	0.00
80	0.00	0.02	0.05	0.04	0.05	0.03	0.02	0.00	0.00	0.00	0.00	0.00
75	0.05	0.13	0.19	0.21	0.22	0.21	0.13	0.03	0.00	0.00	0.00	0.00
70	0.25	0.35	0.42	0.44	0.51	0.52	0.41	0.21	0.03	0.00	0.00	0.12
65	0.60	0.74	0.81	0.91	0.99	1.09	0.89	0.49	0.16	0.04	0.10	0.32
60	1.16	1.43	1.51	1.60	1.77	2.01	1.62	1.00	0.39	0.19	0.30	0.72
55	2.05	2.33	2.44	2.65	2.88	3.11	2.80	1.71	0.81	0.42	0.62	1.36
50	3.31	3.65	3.83	4.16	4.48	4.72	4.15	2.79	1.43	0.82	1.16	2.41
45	4.95	5.22	5.48	5.80	6.30	6.58	5.49	4.09	2.37	1.45	1.92	3.90
40	7.06	7.24	7.71	8.52	9.24	9.43	7.74	5.46	3.62	2.19	2.96	5.52
35	9.75	9.83	10.82	11.15	11.63	11.35	9.42	7.70	5.08	3.31	4.33	8.42
30	11.58	11.87	12.82	13.97	14.04	13.29	11.61	9.77	6.74	4.29	5.78	10.66
25	13.30	13.91	14.72	15.51	15.34	14.31	12.89	11.60	9.29	5.86	8.24	12.18
20	14.21	14.89	15.80	16.61	16.27	15.08	13.73	12.63	10.86	7.40	10.01	13.12
15	14.63	15.45	16.47	17.30	16.86	15.63	14.40	13.43	11.99	8.96	11.70	13.62
10	14.65	15.58	16.74	17.60	17.14	15.96	14.90	14.04	12.91	11.05	12.40	13.77
5	14.29	15.30	16.61	17.51	17.09	16.06	15.21	14.44	13.53	12.20	12.75	13.62
0	13.60	14.65	16.10	17.03	16.72	15.90	15.30	14.63	13.83	12.78	12.85	13.20
-5	12.66	13.70	15.24	16.18	16.02	15.43	15.12	14.60	13.91	12.98	12.74	12.58
-10	11.50	12.51	14.07	14.94	14.94	14.61	14.63	14.34	13.80	12.97	12.46	11.77
-15	10.12	11.09	12.49	13.28	13.38	13.36	13.77	13.83	13.51	12.78	12.02	10.86
-20	8.45	9.32	10.34	10.80	10.73	10.72	12.47	13.06	13.04	12.42	11.45	9.61
-25	7.03	7.71	8.21	7.47	7.61	8.50	9.87	11.72	12.39	11.94	10.68	8.45
-30	5.79	5.92	5.61	5.23	5.29	5.81	7.81	8.85	11.54	11.34	9.87	7.18
-35	4.59	4.33	4.14	3.48	3.37	4.17	5.51	7.81	9.81	10.57	8.91	6.39
-40	3.78	3.45	2.91	2.14	2.07	2.63	4.06	5.45	8.11	9.51	7.86	5.58
-45	3.11	2.50	1.94	1.27	1.09	1.50	2.64	4.15	6.01	8.49	7.14	4.51
-50	2.47	1.91	1.32	0.69	0.52	0.80	1.61	2.91	4.54	6.59	5.85	3.70
-55	1.93	1.40	0.78	0.36	0.20	0.35	0.93	1.94	3.29	4.61	4.38	2.97
-60	1.52	1.02	0.49	0.10	0.03	0.14	0.47	1.18	2.26	3.57	3.42	2.37
-65	1.13	0.67	0.28	0.03	0.00	0.02	0.23	0.72	1.51	2.33	2.38	1.76
-70	0.80	0.45	0.14	0.00	0.00	0.00	0.06	0.37	0.89	1.43	1.57	1.25
-75	0.54	0.27	0.05	0.00	0.00	0.00	0.02	0.22	0.50	0.82	0.94	0.76
-80	0.30	0.14	0.03	0.00	0.00	0.00	0.00	0.07	0.28	0.43	0.48	0.43
-85	0.17	0.07	0.03	0.00	0.00	0.00	0.00	0.06	0.13	0.20	0.20	0.18
-90	0.05	0.05	0.05	0.05	0.05	0.05	0.04	0.04	0.04	0.04	0.04	0.04